Eigenvalues and eigenfunctions of billiards in a constant magnetic field

M. A. M. de Aguiar
Instituto de Física ''Gleb Wataghin,'' Universidade Estadual de Campinas, Campinas 13083-970, São Paulo, Brazil
(Received 30 May 1995; revised manuscript received 30 November 1995)

We present a simple and efficient numerical method to compute the eigenvalues and eigenfunctions of two-dimensional billiards subjected to a constant magnetic field in the perpendicular direction. As examples we present results for the circular billiard, where the method is particularly simple, and for the square billiard, which is nonintegrable for nonzero fields.

PACS number(s): 05.45.+b, 03.65.Ge

I. INTRODUCTION

In the last few years there has been an increasing interest in the behavior of confined electrons subjected to a uniform magnetic field. From the classical point of view, this subject has a long history that starts with the work of Robnik and Berry [1] and can be traced to the paper of Berglund and Kunz [2]. The recent experiment of Levy *et al.* [3] has also motivated several theoretical analyses from the quantum mechanical point of view [4–7]. These were mainly concerned with the semiclassical behavior of the magnetic susceptibility of an ensemble of noninteracting electrons at low temperatures. The connection with the quantum Hall effect, where there is an additional electric field in the plane of the electrons, is also evident and of great importance [8,9].

If the confining potential is that of a billiard, i.e., zero inside a domain $\mathscr{B}$ and infinite outside, then, for zero magnetic field, the motion is along straight lines with specular reflections at the boundary $\partial\mathscr{B}$. In this case, the classical dynamics can be completely described by looking only at successive collisions of the particle with the boundary, since the motion is otherwise trivial. This simplified view is realized by the *bouncing map*, that gives the arc length along the boundary where the collision occurs versus the cosine of the angle with which the particle leaves towards the next collision. The quantum mechanical analogues of this simplification are the so-called *boundary methods*, which also reduce the calculation of eigenvalues and wave functions to a problem involving $\partial\mathscr{B}$ only.

If the magnetic field B is nonzero, a particle of unity mass and charge moves along arcs of circles of radius ($c=1$) $R=\sqrt{2E}/B$, where E is the particle energy, also reflecting specularly at the boundary. Therefore, if B is large enough, there will be orbits that never touch the boundary, and, in this case, the bouncing map cannot represent the classical dynamics completely. This could induce one to the conclusion that quantum mechanical boundary methods should not apply in such a situation. In this paper we show that this is, however, not true.

Some previous numerical examples of particles in perpendicular magnetic fields have been considered either for simple billiard shapes [10], or for smooth potentials in weak magnetic fields [7]. A very detailed quantum mechanical study has also been presented for the case of a single line of magnetic flux threading the billiard, the so-called Aharonov-Bohm billiards [11,12]. The general case of a billiard in a constant uniform magnetic field of arbitrary strength has, however, not yet been tackled succesfuly. The aim of this paper is to develop a method to treat such a general case.

The method we present here is based on the fact that the solutions for the two-dimensional Hamiltonian $H=\frac{1}{2}(\mathbf{p}-e/c\mathbf{A})^2$ with $\boldsymbol{\nabla}\times\mathbf{A}=B\hat{\mathbf{z}}$ are well known in the open space. Since the eigenfunctions are highly degenerated, a proper linear combination that vanishes on a given boundary can be found for some discrete values of the energy. The idea is, therefore, to reduce the calculation of the coefficients of such an expansion to a linear set of equations involving only the billiard boundary. We emphasize, however, that this procedure is not equivalent to the so-called *boundary integral equation method* [13], largely used in the solution of the Helmholtz equation [14], where one makes use of the Green's function to derive an equation where only the normal derivative of the wave function ψ at the boundary is necessary. Here, although we compute ψ only at the boundary, we need a formal expansion of ψ that is valid in the whole space. Similar methods are common in scattering theory and have also been used recently to compute eigenvalues of billiards (see, for instance, [15], and references therein).

This paper is organized as follows: in Sec. II we motivate our basic procedure by looking first at the case of zero magnetic field. In Sec. III we show how to extend it to the case of a constant magnetic field and in Sec. IV we present numerical results for the circle and square billiards. We compare these results with those obtained by direct diagonalization the Hamiltonian in the basis of field-free problem (which works well for weak fields) and find very good agreement. Contour levels of the probability density are also displayed for a few states to illustrate the calculation of the eigenfunctions.

II. FREE BILLIARDS

In this section we are going to motivate our numerical method by looking first at billiards with no external fields. The two-dimensional free particle Hamiltonian operator $H=\frac{1}{2}p^2$ written in polar coordinates reads

$$H=-\frac{\hbar^2}{2}\left[\frac{1}{r}\frac{\partial}{\partial r}\left(r\frac{\partial}{\partial r}\right)+\frac{1}{r^2}\frac{\partial^2}{\partial\theta^2}\right]. \tag{1}$$

The solutions of the time-independent Schrödinger equation $H\psi = E\psi$ that are regular at the origin are given by $\Psi(r,\theta) = J_m(kr)e^{im\theta}$, where $J_m(x)$ are integer Bessel functions and $E = k^2/2$. Since the eigenvalue is independent of m, the most general eigenfuntion of eigenvalue E is

$$\Psi(r,\theta) = \sum_m C_m J_m(kr) e^{im\theta}. \tag{2}$$

If we now confine the particle to a billiard $\mathscr{B}$ containing the origin, the eigenfunctions will be given by specific linear combinations such as Eq. (2) such that $\Psi(r,\theta)|_{\partial\mathscr{B}} = 0$, where $\partial\mathscr{B}$ is the billiard boundary. Of course, despite the infinite number of functions entering in Eq. (2), such a condition can only be fulfilled for some discrete values of k.

A numerical algorithm to compute the eigenenergies can be implemented as follows: take a discrete set of N points along the boundary, then, rewriting Eq. (2) in terms of sines and cosines, we get

$$\Psi(r_j,\theta_j) = \sum_{m=1}^{M} J_m(kr_j)[C_m \cos m\theta + D_m \sin m\theta] + C_0 J_0(kr_j) = 0 \tag{3}$$

for all $(r_j,\theta_j) \in \partial\mathscr{B}$. Choosing $2M+1 = N$, we get a set of homogeneous linear equations whose nontrivial solution exists if

$$\det S(k) = 0, \tag{4}$$

where

$$S(k) = \begin{pmatrix} J_0(kr_1) & J_1(kr_1)\cos\theta_1 & J_1(kr_1)\sin\theta_1 & \cdots & J_M(kr_1)\cos M\theta_1 \\ \vdots & \vdots & \vdots & & \vdots \\ J_0(kr_N) & J_1(kr_N)\cos\theta_N & J_1(kr_N)\sin\theta_N & \cdots & J_M(kr_N)\cos M\theta_N \end{pmatrix}. \tag{5}$$

Plotting $\det(S)$ as a function of k provides a nice way to compute the eigenvalues. It is important to notice that this procedure fails at a degenerated eigenvalue, since the determinant ''changes sign twice'' at the same point. Therefore, if the billiard has symmetries, they should be separated before the method is applied. We have tested this numerical method for the case of a square billiard and computed the first 30 energy levels using about 15 points along each side of the square. The results obtained were accurate up to the sixth significant figure. In the next section we shall show how this method can be extended to include a magnetic field in the z direction.

III. BILLIARDS IN A MAGNETIC FIELD

A. The Schrödinger equation for a constant uniform field

The Hamiltonian describing a particle of unity mass and charge moving on the x-y plane and subjected to a magnetic field $\mathbf{B}$ in the z direction is given by $(c=1)$

$$H = \tfrac{1}{2}(\mathbf{p} - \mathbf{A})^2, \tag{6}$$

where the vector potential $\mathbf{A}$, satisfying $\boldsymbol{\nabla}\times\mathbf{A} = B(x,y)\hat{\mathbf{z}}$, is defined up to the gradient of an arbitrary function. In the case of a constant uniform magnetic field, $B(x,y) = B_0$, it is usual to choose the Landau gauge $\mathbf{A}_L = -B_0 y\hat{\mathbf{x}}$. It leads to the well-known Landau wave functions ψ_L, which are simultaneous eigenfunctions of H and p_x, localized in the y direction but not in the x direction, where it behaves like a plane wave [16]. The eigenenergies, or Landau levels, are given by

$$E_{kn} = \hbar B(n + 1/2) \tag{7}$$

and are constinuously degenerated, since they are independent of the p_x eigenvalue $\hbar k$.

Although the Landau gauge is the most usual choice for the vector potential, in this paper we shall work with the *symmetric gauge* $\mathbf{A}_s = B_0/2(-y\hat{\mathbf{x}} + x\hat{\mathbf{y}})$, for reasons to be explained below. Then the Hamitonian assumes a simple form in polar coordinates and reads

$$H = \frac{1}{2}\left(p_r^2 + \frac{L_z^2}{r^2}\right) + \frac{\omega^2 r^2}{2} + \omega L_z, \tag{8}$$

where

$$p_r^2 = -\frac{\hbar^2}{r}\frac{\partial}{\partial r}\left(r\frac{\partial}{\partial r}\right),$$

$$L_z = -i\hbar\frac{\partial}{\partial\theta},$$

and $\omega = \omega_c/2 = B/2$ is half the cyclotronic frequency.

This time it is the z component of the angular momentum that commutes with H. Writing [17]

$$\psi_s(r,\theta) = e^{im\theta} u^{|m|/2} e^{-u/2} f_m(u), \tag{9}$$

where $u = r^2 B/2\hbar \equiv (r/b_s)^2$, we find that f satisfies

$$u\frac{d^2 f}{du^2} + (|m| + 1 - u)\frac{df}{du} + \alpha f = 0 \tag{10}$$

with

$$\alpha \equiv \frac{E - (m + |m| + 1)}{2\hbar\omega}. \tag{11}$$

Equation (11) can be recognized as the differential equation satisfied by the confluent (or degenerated) hypergeometric function $\Phi(-\alpha,|m|+1,u)$ [16,18], whose regular solution is given by the series

$$\Phi(a,c,u)=1+\frac{a}{c}\frac{u}{1!}+\frac{a(a+1)}{c(c+1)}\frac{u^2}{2!}+\cdots. \tag{12}$$

When the series is truncated, to ensure that ψ_s goes to zero as u goes to infinity, α is set to an integer and the Landau levels are again obtained. Also, the function Φ becomes a Laguerre polynomial and ψ_s, as opposed to the Landau wave functions ψ_L, becomes well localized. This is the main reason for choosing the symmetric gauge.

B. The boundary condition

Let us now confine the charged particle to a billiard $\mathscr{B}$ containing the origin. In analogy to the procedure described in Sec. II, Eqs. (2)–(5), we could try to combine several degenerated eigenfunctions, Eq. (9), and find the billiard eigenenergies by imposing that these linear combinations go to zero at the billiard boundary. This, however, would not work here, since, contrary to the situation in Sec. II, the Landau levels are discrete and, therefore, cannot be scanned continuously. Also, including in the linear combination eigenfunctions of different eigenenergies would not help, since, by construction, this cannot produce an eigenfunction of the same Hamiltonian operator.

The solution to this difficulty is to allow for unbounded wave functions: the behavior at infinity will not be relevant if we are going to look only at the finite area enclosed by the billiard boundary. For the asymmetric solution this implies considering the full *untruncated* Hermite series. For the symmetric case, which is more attractive because of the localization of the wave functions, the solution becomes

$$\psi_s^{\alpha m}(r,\theta)=e^{im\theta}(r/b_s)^{|m|}e^{-r^2/(2b_s^2)}\Phi(-\alpha,|m|+1,r^2/b_s^2) \tag{13}$$

and the eigenenergies

$$E_{\alpha m}=2\hbar\omega\left(\alpha+\frac{m+|m|}{2}+\frac{1}{2}\right), \tag{14}$$

where α varies continuously. The wave functions $\psi^{\alpha_m,m}$ (we are omitting the subscript s) with

$$\alpha_m=\begin{cases}\alpha_0\equiv E/(2\hbar\omega)-1/2 & \text{if } m\leqslant 0\\ \alpha_0-m & \text{if } m\geqslant 1\end{cases} \tag{15}$$

are all degenerated with energy E. Therefore, the linear combination

$$\psi_E(r,\theta)=\sum_{m=-\infty}^{\infty}C_m e^{im\theta}(r/b_s)^{|m|}e^{-r^2/(2b_s^2)} \times\Phi(-\alpha_m,|m|+1,r^2/b_s^2) \tag{16}$$

is the analogue of Eq. (2). Notice that here the complex exponential $e^{im\theta}$ cannot be split into sines and cosines, since $\psi^{\alpha_m,m}$ and $\psi^{\alpha_{-m},-m}$ have different energies. Of course this intrinsic complex character is a consequence of the magnetic field. Notice also that there is no *a priori* impediment to using negative values of α. Truncating the sum over the m's from m_i to m_f we are left with m_f-m_i+1 coefficients, which we should determine using exactly $N=m_f-m_i+1$ points (r_n,θ_n) along the billiard boundary and imposing that ψ_E go to zero at these points. The only difference is that now the resulting determinant is complex and both its real and imaginary parts should go to zero at the correct eigenvalue. Writing this boundary condition explicitly gives

$$\sum_{m=m_i}^{m_f}C_m e^{im\theta_n}(r_n/b_s)^{|m|}e^{-r_n^2/(2b_s^2)}\Phi(-\alpha,|m|+1,r_n^2/b_s^2)=0 \tag{17}$$

for $n=1,2,\ldots,N$, whose nontrivial solution is given by the condition

$$\det S(E)=0, \tag{18}$$

where

$$S(E)=\begin{pmatrix}\phi_{\alpha_{m_i},m_i}(r_1)e^{im_i\theta_1} & \cdots & \cdots & \phi_{\alpha_{m_f},m_f}(r_1)e^{im_f\theta_1}\\ \vdots & \vdots & & \vdots\\ \phi_{\alpha_{m_i},m_i}(r_N)e^{im_i\theta_N} & \cdots & \cdots & \phi_{\alpha_{m_f},m_f}(r_N)e^{im_f\theta_N}\end{pmatrix} \tag{19}$$

and

$$\phi_{\alpha,m}(u)=u^{|m|/2}e^{-u/2}\Phi(-\alpha,|m|+1,u). \tag{20}$$

Once an eigenenergy E has been found, we can go back to Eq. (16) and solve it for the coefficients C_m. This determines the eigenfunctions and completes the calculation. In the next subsection we discuss the behavior of the function Φ and the choices of m_i and m_f.

C. The function Φ and the sum over the *m*'s

The confluent hypergeometric function Φ can be computed easily from its series, Eq. (12). Figure 1 shows a numerical example where, instead of plotting Φ itself, we show the behavior of the radial part of the wave function, $\phi(u)$, Eq. (20). When α is an integer n (solid curve), Φ is a polynomium and $\phi(x)$ goes to zero as $u\to\infty$. For slightly larger (smaller) values of α, $\phi(u)$ goes to $+\infty$ $(-\infty)$ if n is odd. If n is even the behavior at infinity changes sign. The

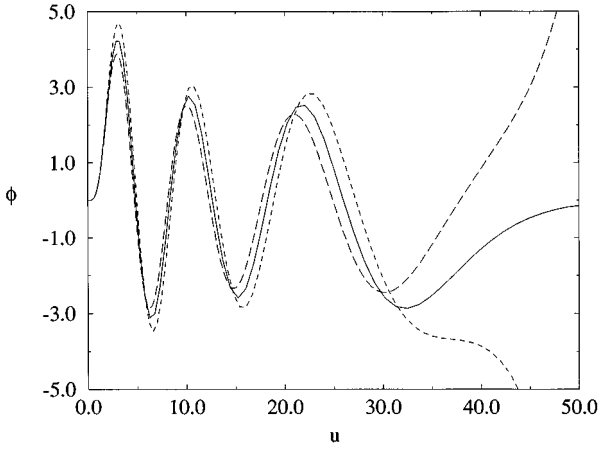

FIG. 1. Behavior of the radial part of the wave function as given by Eq. (20) for $m=9$. The solid line corresponds to $\alpha=5.0$, the short-dashed line to $\alpha=4.8$, and the long-dashed line to $\alpha=5.2$.

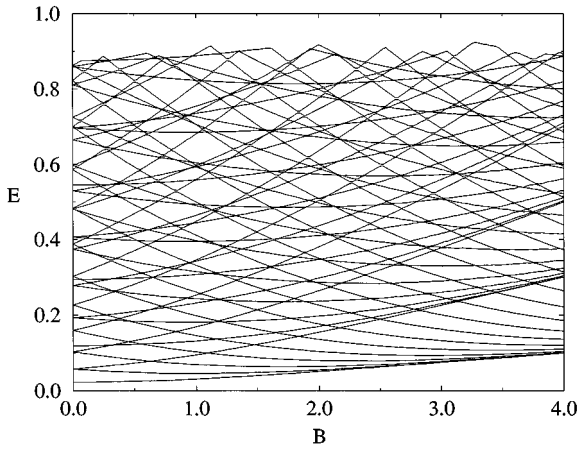

FIG. 2. First 50 eigenvalues of the circular billiard as a function of the magnetic field B for $\hbar=0.05$.

number of zeros of ϕ is determined by the integer part of α. If α is negative (the argument of Φ is positive) then there are no zeros.

For a fixed value of the energy E and $\alpha_0=E/(2\hbar\omega)+1/2$, we see that, as $m\to\infty$, $\Phi\to 1$. For positive m's, we have $\alpha_m+m=\alpha_0$ and $\Phi(m-\alpha_0,m+1,u)\to e^u$. Then, as $|m|\to\infty$

$$\phi_{\alpha_m,m}(u)\to\begin{cases} u^{|m|/2}e^{-u/2} & \text{if } m<0 \\ u^{m/2}e^{u/2} & \text{if } m>0 \end{cases}$$

and, since our wave function has to go to zero at the boundary, we expect it to have no components on large $|m|$'s, either positive (because ϕ goes to zero if $u<1$ and to infinity if $u>1$) or negative (because ϕ is nonzero only near $u\simeq\sqrt{m}\to\infty$). This indicates that the expansion (16) is a good representation of the wave function.

One important guide to the numerical calculations is the counting function $N(E)\equiv\Sigma\Theta(E-E_n)$, whose classical limit (or Weyl term) for billiards is $N_w(E)=\mathscr{A}E/(2\pi\hbar^2)$, where $\mathscr{A}$ stands for the area enclosed by $\partial\mathscr{B}$. This expression is also valid for billiards in perpendicular magnetic fields. Therefore, when scanning the determinant (19) as a function of the energy, it might happen that a pair of levels that lie close together is missed by the computation. This lack of levels will be felt immediately by $N(E)$, indicating that a finer scanning should be made in that region.

It is not very easy to estimate how many m's, or points along the boundary, are actually needed to achieve a good convergence of the eigenvalues. In the case of the square billiard we have used approximately 20 points on each side of the square. To test the accuracy of the numerical results one should first redo the calculations using a slightly increased number of points and compare the results with the previous computation. Also, and this turns out to be a crucial test, one should check whether the real and imaginary parts of the determinant (19) go to zero at the same point. Therefore, when scanning the energy at steps of ΔE, if one finds that both $\mathrm{Re}[\det(S)]$ and $\mathrm{Im}[\det(S)]$ change sign between two consecutive points, one should refine the energy grid, making $\Delta E\to\Delta E/2$, for instance, and see to what precision they keep passing through zero in the same interval. In any case, however, there is always an optimum number of basis functions to be used. If we use much more than this, the contribution of these extra states to the wave function might be so small that we introduce lines of nearly zeros in our determinant, spoiling the numerical convergence.

IV. NUMERICAL RESULTS

In this section we apply the method just developed to two model problems: the circular and the square billiards. In the circular billiard the angular momentum is still a good quantum number and the classical problem is also integrable. For the square billiard, on the other hand, the geometry seems to be one of the most inappropriate to work with circular functions. Even in this case, however, the method works well.

A. The circular billiard

The circular billiard is an almost trivial case, since the problem is separable in cylindrical coordinates. A previous theoretical analysis of this problem has been presented by Rensink [19]. The calculation of the eigenvalues is reduced to find the zeros of the confluent hypergeometric function and, therefore, can be said to be *exact*. In this respect the calculation is very much like that of the zero-field case, where we have to find the zeros of Bessel functions. Setting the billiard radius to $1/\sqrt{\pi}$, so as to have unity area, we have the equation

$$\Phi(-\alpha,|m|+1,B/(2\pi\hbar))=0, \tag{21}$$

which should be solved for α. The eigenenergies are then given by Eq. (14). Notice that since Eq. (21) depends only on $|m|$, for each α there will be two states associated, the one with negative m having the lowest energy. Also, the separability of the problem implies that the energies will exhibit level crossings when the magnetic field is varied. We have computed the first 100 eigenstates from $B=0$ to $B=4$ at steps of 0.025. In Fig. 2 we show the first 50 eigenvalues. For B around 3 or 4 and low energies, we can see very neatly the levels clustering into the Landau levels. As we go to higher energies we notice a few gaps between the levels.

These gaps are a numerical artifact due to the rapid increase in the density of level crossings with the energy. They disappear with a finer grid in B.

B. The square billiard

The square billiard with a nonzero magnetic field is nonintegrable, since the angular momentum is not conserved between consecutive bounces of a trajectory with the boundary. The important classical parameter is not the energy E nor the magnetic field B, but the radius $R=\sqrt{2E}/B$. Here, as in the previous example, we set the billiard area equal to 1.

Although the purpose of this paper is to describe a numerical method for doing quantum mechanical calculations, it is instructive to look first at the classical behavior to understand the quantum output in the light of semiclassical theory. In Fig. 3 we show the bouncing map, i.e., the map between consecutive collisions with the boundary, for $R=2.0$, $R=1.0$, and $R=0.5$. In this figure the x axis shows the arc length s along the boundary where the collision occurs counted from the lower left corner of the square, and the y axis shows p, the cosine of the angle between the tangent of the trajectory just after the collision and the corresponding side of the square. Although the x axis should go from zero to four, we show only the part from 0 to 1, since the other quarters are similar.

For $R>0.5$ all trajectories necessarily hit the boundary and the bouncing map is a complete representation of the dynamics. For $R<0.5$, however, a fraction $(1-2R)^2$ of the trajectories stay circling inside the square, never touching the boundary. This same fraction of phase space is, therefore, completely regular and does not show up in the bouncing map. From Fig. 3 we see that the magnetic field has a very strong effect on the classical dynamics and it acts in a complicated way: the limits $R\rightarrow 0$ and $R\rightarrow\infty$ are both integrable [1,2] and in the interval in which $0.4\leqslant R\leqslant 20$, the regular portion of phase space oscillates as R changes. Therefore, we expect to find both neat level repulsion and very narrow avoided crossings for intermediate values of B.

The quantum mechanical calculations can be performed in two different ways: the first option is to use the wave functions of the zero-field problem, which have the correct boundary condition, as a basis to diagonalize the matrix with non-zero B. The second option is to use the method developed in the previous section. For low values of the magnetic field both methods work and their results can be compared. For high values of B, however, the diagonalization is very poor while our procedure works even better. We emphasize that the diagonalization procedure is possible only if the zero-field wave functions are known before-hand, otherwise these wave functions *and* the matrix elements would have to be computed numerically before the diagonalization.

Before we display the results of the numerical calculations, we notice that the symmetry $\theta\rightarrow\theta+\pi/2$ survives the application of the magnetic field. If $\mathscr{U}$ is the operator that rotates by $\pi/2$, then, the eigenfunctions of H are also eigenfunctions of $\mathscr{U}$ with eigenvalues $u=1$, i, -1, and $-i$. Therefore, the m's in Eqs. (16) and (17) are multiples of 4, being 0, 1, 2, or 3mod(4), respectively. For $B=0$ the levels for $u=1$, for example, are $\pi^2\hbar^2(n^2+m^2)/2$ with (n,m) both odd [with (n,m) or (m,n) counting as a single level], or both even with $n\neq m$. For very large B and low energies, on the other hand, the levels should cluster at the Landau levels $\hbar B(n+1/2)$ with a degeneracy of $B/(2\pi\hbar)$.

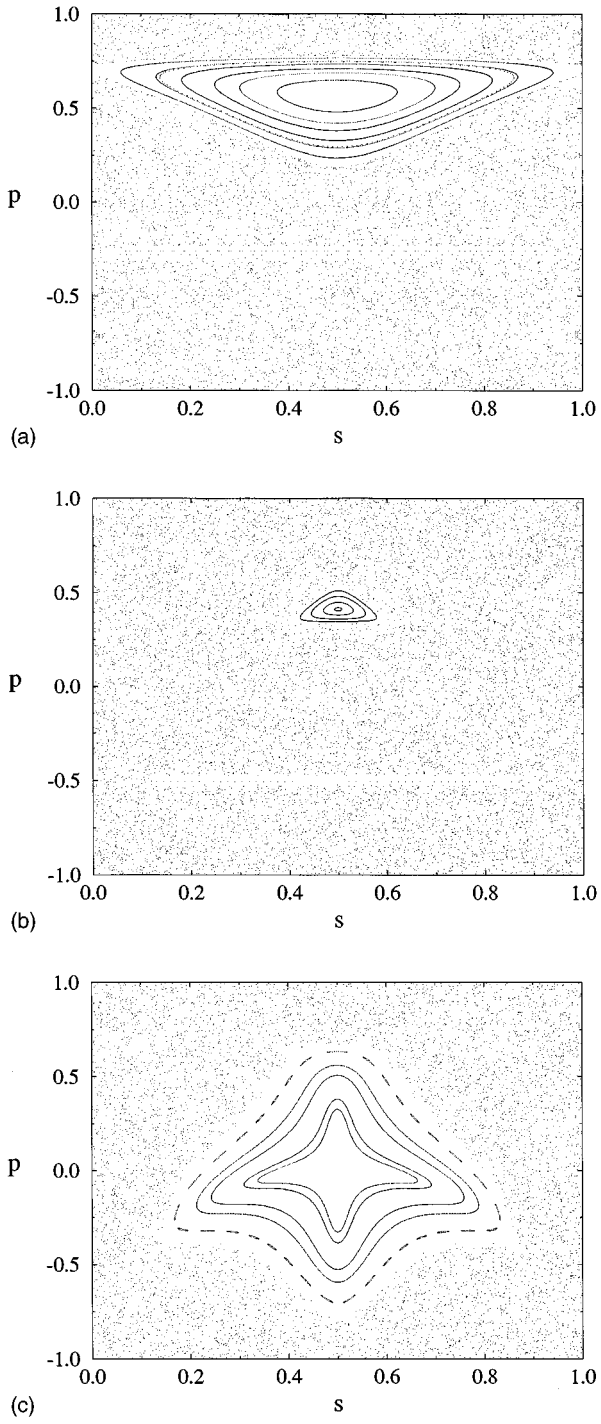

FIG. 3. Bouncing map for the square billiard for (a) $R=2.0$; (b) $R=1.0$, and (c) $R=0.5$.

We have computed the first 30 eigenenergies for the symmetry class $u=1$ for B in the interval 0 to 4 at steps of 0.1 as shown in Fig. 4. The thick dotted lines are curves of constant R, whose value is written close to the corresponding curve. We see from this figure that, as expected from the classical bouncing map, the energy levels present some very narrow avoided crossings, probably due to the presence of the large

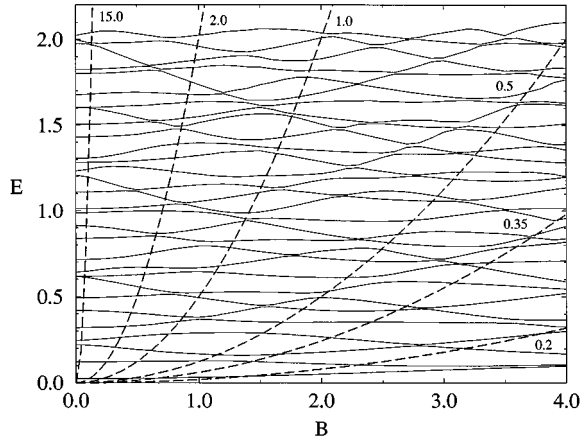

FIG. 4. First 30 eigenvalues of symmetry $u=1$ for the square billiard as a function of the magnetic field B for $\hbar=0.05$. The thick dashed lines are curves of constant classical radius, $E=R^2B^2/2$. The numbers close to each curve denote the corresponding value of R.

stability island of the lozenge orbit that persists for a wide range of B's. In Fig. 5 we display the relative error (times 10^4)in the calculations at $B=0.2$, $(E_n^{\rm diag}-E_n)/E_n^{\rm diag}$ where E_n are obtained with the method proposed here and $E_n^{\rm diag}$ are obtained by diagonalizing a 307×307 matrix (including only the $u=1$ symmetry class) and find very good agreement. Similar comparisons at $B=1.0$ and $B=4.0$ give errors of the same order of magnitude.

From the point of view of computational time, at $B=0.2$ the diagonalizations are very efficient and a 307×307 matrix leads to a total of 150 eigenvalues converged with 4 figures of precision (counting only the $u=1$ symmetry class). This takes around 4 min of CPU in a Digital AlphaStation 250. An equivalent computation with the method of this paper would take about 10 min. At $B=4.0$, however, a 900×900 diagonalization would furnish only around 50 eigenvalues with the same precision and would take about 2 h of CPU (remember that the matrices are complex). The application of our method, on the other hand, is not very sensitive to B and would take only a few minutes to compute the eigenvalues.

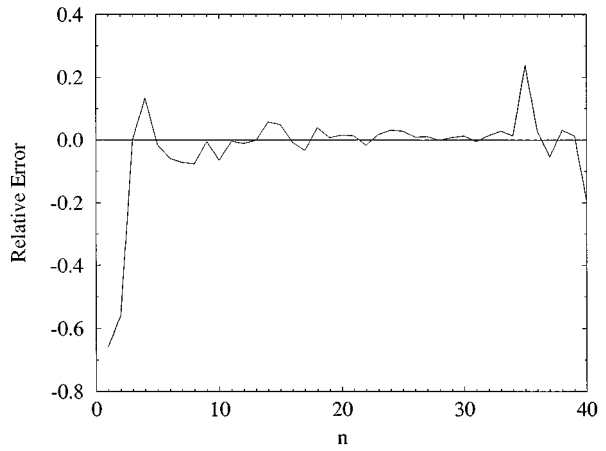

FIG. 5. Relative error times 10^4 between a 307×307 diagonalization and the method of this paper for the first 40 levels of symmetry $u=1$ at $B=0.2$.

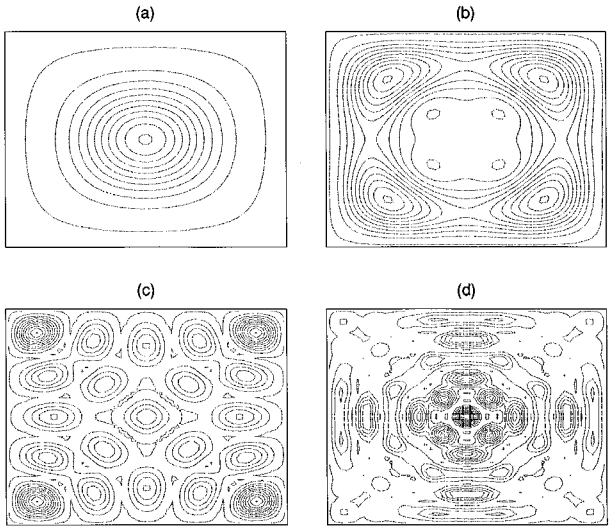

FIG. 6. Contour levels of $|\psi(\mathbf{r})|^2$ for the eigenstates number 1 (a), 2 (b), 7 (c), and 25 (d) at $B=2.0$. The eleven contour lines shown in each figure are 0.99, from 0.8 to 0.1 at steps of 0.1 and 0.01 of the maximum probability density.

Figure 6 shows the probability density $|\psi|^2$ for some eigenstates at $B=2.0$ computed as described at the end of Sec. III B. Parts (a) and (b) show the first and second eigenstates, respectively. Parts (c) and (d) show states number 7 and 25 where the *scar* of the lozenge orbit is visible.

V. CONCLUSIONS

We have presented a numerical method to compute eigenvalues and eigenfunctions of billiards in a constant magnetic field. As numerical examples we have examined the two important cases of the circle and the square billiards. The circular billiard is particularly simple and the method reduces to find the zeros of the hypergeometric confluent function. For other geometries we combine these functions and impose that the wave function go to zero at the boundary. For simple cases like the square, the eigenfunctions for zero magnetic field are known analytically and could also be used as a basis to diagonalize the Hamiltonian operator. The convergence, however, tends to decrease very fast as the field strength increases. For more complicated (nonintegrable) cases the diagonalization procedure becomes very hard, since a first numerical calculation to get the zero field basis is necessary. The method proposed here works well for all values of the magnetic field, except very close to zero, where the width $b=\sqrt{2\hbar/B}$ has a singularity. It is important to emphasize that the square billiard is perhaps one of the most complicated cases for the application of this method, since we are using circular hypergeometric functions to adjust functions that go to zero at a square. We believe that ellipses and conformal maps of the circle, for instance, would produce even better results.

An interesting point that comes about with this method is the fact that, although the bouncing map cannot represent completely the dynamics of these systems if the magnetic field is too intense, since there will be a considerable fraction of orbits that never touch the boundary, the quantum mechanical problem can still be reduced to a boundary problem.

In that case the solutions with nearly integer α's are selected, since this is the only way to avoid a blowup of the wave function. Therefore, quantum mechanically, the boundary is always *seen* by the wave function, even if it recedes to infinity.

ACKNOWLEDGMENTS

It is a pleasure to thank A.M. Ozorio de Almeida, F. Bensch, and M.L. Tiago for fruitful suggestions. This paper was partly supported by CNPq, FAPESP, and FINEP.

[1] M. Robnik and M.V. Berry, J. Phys. A **18**, 1361 (1985); M. Robnik, in *Nonlinear Phenomena and Chaos*, edited by S. Sakar (Adam Hilger, London, 1986), p. 303.
[2] N. Berglund and H. Kunz, J. Stat. Phys. (to be published).
[3] L.P. Lévy, D.H. Reich, L. Pfeiffer, and K. West, Physica B **189**, 204 (1993).
[4] D. Ullmo, K. Richter, and R. Jalabert, Phys. Rev. Lett. **74**, 383 (1995).
[5] F. von Oppen, Phys. Rev. B **50**, 151 (1994).
[6] O. Agam, J. Phys. (France) I **4**, 697 (1994).
[7] S.D. Prado, M.A.M. de Aguiar, J.P Keating, and R. Egydio de Carvalho, J. Phys. A **27**, 6091 (1994).
[8] *The Quantum Hall Effect*, edited by R.E. Prange and S.M. Girvin (Springer-Verlag, New York, 1990).
[9] S.A. Trugman, Phys. Rev. Lett. **62**, 579 (1989); V. Nikos Nicopoulos and S.A. Trugman, Phys. Rev. B **45**, 11 004 (1992); U. Sivan, Y. Imry, and C. Hartzstein, *ibid.* **39**, 1242 (1989).
[10] K. Nakamura and K. Thomas, Phys. Rev. Lett. **61**, 247 (1988).
[11] M.V. Berry and M. Robnik, J. Phys. A **19**, 649 (1986); M. Robnik and M.V. Berry, *ibid.* **19**, 669 (1986).
[12] G. Date, S.R. Jain, and M.V.N. Murthy, Phys. Rev. E **51**, 198 (1995).
[13] R.J. Riddel, J. Comput. Phys. **31**, 21 (1979); **31**, 42 (1979); R.E. Kleimann and G.F. Roach, SIAM Rev. **16**, 214 (1974).
[14] S.W. McDonnald and A.N. Kaufmann, Phys. Rev. Lett. **42**, 1189 (1979); Phys. Rev. A **37**, 3067 (1988); Y.Y. Bai, G. Hose, K. Stefanski, and H.S. Taylor, *ibid.* **31**, 2821 (1985); E.J. Heller, Phys. Rev. Lett. **53**, 1515 (1984); E.J. Heller, P.W. O'Connor, and J. Gehlen, Phys. Scr. **40**, 354 (1989); M.V. Berry, Ann. Phys. (N.Y.) **131**, 163 (1981); E. Bogomolny, Comments At. Mol. Phys. **25**, 67 (1990); A.M. Ozorio de Almeida, J. Math. Phys. A **27**, 2891 (1994).
[15] C. Rouvinez and U. Smilansky, J. Phys. A **28**, 77 (1995).
[16] L.D. Landau and L. Lifshitz, *Quantum Mechanics (Non-Relativistic Theory)* (Pergamon, New York, 1977).
[17] C. Cohen-Tannoudji, B. Diu, and F. Laloe, *Quantum Mechanics* (Wiley, New York, 1977), Vol. 1.
[18] A. Erdelyi *et al.*, *Higher Transcendental Functions* (McGraw-Hill, New York, 1953), Vol. 1.
[19] M.E. Rensink, Am. J. Phys. **37**, 900 (1969).